LIMNOLOGY
and
OCEANOGRAPHY

ASLO

Limnol. Oceanogr. 9999, 2019, 1–12

doi: 10.1002/lno.11249

Vegetation recovery on neighboring tidal flats forms an Achilles' heel of saltmarsh resilience to sea level rise

Zhenchang Zhu,[1,2*] **Jim van Belzen**,[1] **Qin Zhu**,[2] **Johan van de Koppel**,[1] **Tjeerd J. Bouma**[1,3]

[1]Department of Estuarine and Delta Systems, Royal Netherlands Institute for Sea Research and Utrecht University, Yerseke, The Netherlands
[2]Institute of Environmental and Ecological Engineering, Guangdong University of Technology, Guangzhou, China
[3]Faculty of Geosciences, Department of Physical Geography, Utrecht University, Utrecht, The Netherlands

Abstract

Coastal wetlands such as saltmarshes are valued as prominent buffering ecosystems to global climate change and sea level rise (SLR), yet their long-term persistence may also be threatened by these global change stressors. While saltmarshes are increasingly thought to be resilient to SLR owing to high vertical marsh adaptability, their long-term stability remains uncertain due to our poor understanding of marsh resilience at the marsh-tidal flat interface, where wave disturbance can progressively shift vegetated marsh toward a bare tidal flat state. Here, we explore how SLR affects vegetation recoverability on tidal flats using cordgrass, a globally common saltmarsh foundation species, as a model plant. Combined field and model results demonstrate that small increases in wave forcing due to raised water depth over tidal flats can dramatically weaken or even block vegetation recovery from eroding marsh edges, through hampering seed persistence. Vegetation recovery on tidal flats next to the marsh edge thus represents an unrecognized Achilles' heel of marsh resilience to SLR, which if ignored may cause underestimation of marsh vulnerability. These findings are highly relevant for a more comprehensive assessment of marsh susceptibility to SLR in systems where seeds play an essential role in revegetation of tidal flats, and highlight the importance of maintaining either a wave-protected or well-elevated tidal flat near the marsh edge that allows for quick vegetation recovery for supporting resilient marshes.

Coastal wetlands such as saltmarshes are among the most valuable ecosystems on the globe (Costanza et al. 1997), providing many key ecosystem functions such as carbon sequestration and flood protection (Barbier et al. 2011). These features render them prominent ecosystems that naturally buffer the impacts of global climate change as well as sea level rise (SLR) (Duarte et al. 2013; Temmerman et al. 2013). However, SLR also threatens the long-term persistence of coastal wetlands (Kirwan and Megonigal 2013; Wang et al. 2017) and in many cases, its impacts are amplified by local land subsidence caused mainly by human activities (Syvitski et al. 2009). For over 30 yr, there have been widespread concerns about marsh drowning in response to SLR, as this can shift extensive marsh area from the vegetated state to the bare tidal flat state (Kirwan and Megonigal 2013; Kirwan et al. 2016). A recent meta-analysis, however, concludes that—given sufficient sediment—the positive feedback between plant growth and enhanced sedimentation allows most marshes to compensate for SLR (Kirwan et al. 2016). This premise, however, ignores that many marshes face extensive erosion at the marsh edge (van de Koppel et al. 2005; Hughes et al. 2009; Deegan et al. 2012; Silliman et al. 2012; Leonardi et al. 2016), where plant-sediment feedbacks are rendered ineffective. Currently, the knowledge deficit on marsh adaptability in the lateral dimension severely limits our understanding of marsh resilience to SLR.

Lateral marsh losses occur when wave disturbance progressively shifts vegetated marsh toward a bare tidal flat state, often by means of cliff erosion (Allen 2000; van der Wal and Pye 2004; Marani et al. 2011; Leonardi and Fagherazzi 2014). Cliff erosion rate increases linearly with rising wave power and even very small waves may cause erosion of large saltmarsh blocks (Leonardi and Fagherazzi 2014; Leonardi et al. 2016). A resilient marsh will display vegetation recovery and expansion on the tidal flats in front of the retreated marsh (van de Koppel et al. 2005; Bouma et al. 2016). Many meso- and macrotidal marshes have shown cyclic alternations between a marsh retreating phase and a vegetation recovery/expansion phase at the marsh-tidal flat interface on decadal or larger time scales (Allen 2000; van der Wal et al. 2008; Chauhan 2009). Both phases are influenced by wave-induced, erosive dynamics on the tidal flat next to the marsh edge (Bouma et al. 2016; Wang et al. 2017).

*Correspondence: zhenchang.zhu@nioz.nl

Additional Supporting Information may be found in the online version of this article.

Unlike the highly adaptable marsh platform where plants trap sediment and reduce erosion (Kirwan and Megonigal 2013; Kirwan et al. 2016), the adjacent tidal flats are at high risk of becoming increasingly deep due to the rising sea level (Mariotti and Fagherazzi 2010), given the absence of positive plant-sedimentation feedback, the strong sediment competition between the marsh and adjacent tidal flats (Mariotti and Fagherazzi 2010), and worldwide declines of sediment delivery to coasts (Walling and Fang 2003; Syvitski et al. 2009). A numeric marsh-tidal flat coevolution model predicts that, with low sediment availability, a small rate (2 mm yr^{-1}) of SLR may result in up to approximately 30 cm deeper tidal flats after 50 yr, yet without causing significant drowning of adjacent vegetated marsh (Mariotti and Fagherazzi 2010). SLR-increased water depth on adjacent tidal flats allows stronger waves to reach the marsh edge (Mariotti and Fagherazzi 2010; Arns et al. 2017), as a result of reduced bottom friction and relaxed depth limitation. This can increase lateral erosion rates (Mariotti and Fagherazzi 2010; Leonardi et al. 2016; Wang et al. 2017), especially when biotic stressors, e.g., crab burrowing and herbivory, and so on (Holdredge et al. 2009; Hughes et al. 2009) and human activities, e.g., eutrophication and oil spilling, and so on (Deegan et al. 2012; Silliman et al. 2012) weaken erosion resistance at the marsh edge. In this context, whether the marsh can persist in the long run and maintain adequate size for provisioning of key ecosystem services depends critically on a resilient marsh edge that is able to recover from phases of increased edge erosion. Yet, little is known about the consequence of SLR for marsh re-establishment on neighboring tidal flats following lateral retreat of the marsh edge. This knowledge gap significantly impedes comprehensive assessments of marsh susceptibility and accurate predictions of marsh fate under SLR.

Here, we bridge this knowledge gap by examining how SLR-intensified wave forcing shapes seed-based vegetation recovery on adjacent tidal flats (Fig. 1). Seedling establishment is a crucial process of vegetation recovery seen in many meso- and

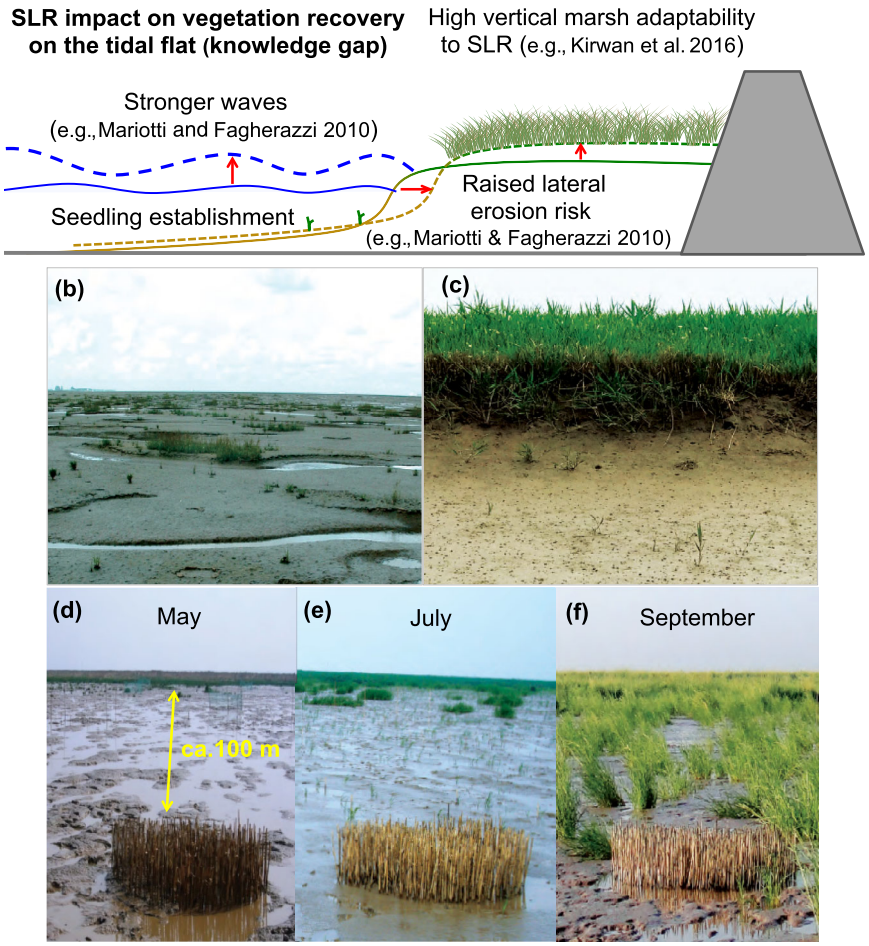

Fig. 1. **(a)** Established knowledge and current knowledge gaps on marsh resilience to SLR and increased wave action. Especially knowledge on the marsh recovery on bare tidal flats is essential for enhancing current understanding of long-term marsh resilience to SLR and associated increase in wave forcing. (**b**) Vegetation development in tidal flats by seedling establishment in Hooge platen, The Netherlands; (**c**) seedling establishment in front of a cliff at a marsh edge in the Yangtze estuary, China; (**d–f**) extensive seedling establishment of smooth cordgrass (*Spartina alterniflora*) lead to rapid vegetation expansion in a marsh in the Yangtze estuary, China.

macrotidal marsh ecosystems around the world (Gray et al. 1991; Temmerman et al. 2007; Strong and Ayres 2013; Liu et al. 2017). Although marsh expansion is in some areas predominantly the result of clonal extension from the existing vegetation (e.g., Allison 1995; Angelini and Silliman 2012), seedling recruitment (Fig. 1b–f) often yields rapid vegetation establishment on tidal flats over extensive areas (Gray et al. 1991; Zhu et al. 2012; Strong and Ayres 2013). Seed-based establishment appears to be especially important in meso- and macrotidal systems where clonal expansion can be halted by the formation of a high cliff at the marsh edge (Fig. 1c), which completely disconnects the tidal flats from the existing vegetation. However, seedling establishment is often constrained by wave disturbance and associated sediment erosion that imposes difficulties for seed persistence (Groenendijk 1986; Marion and Orth 2012; Zhu et al. 2014) and seedling survival (Bouma et al. 2009, 2016; Friess et al. 2012; Balke et al. 2013). Therefore, we hypothesize that SLR-increased wave forcing may undermine marsh resilience at the seaward edge of the marsh where seed colonization is a critical pathway for vegetation recovery.

To test our hypothesis, we combined field measurements and model simulations to quantify the impacts of shifting wave forcing on the ability of the marsh to recover by seed establishment when it has shifted to an unvegetated tidal flat state, using cordgrass (*Spartina* spp.) as a model. Cordgrass globally defines and stabilizes shorelines, laying the foundation for saltmarshes to develop (Strong and Ayres 2013), and seeds often play a critical role in its establishment and range expansion in many parts of the world (Gray et al. 1991; Ayres et al. 2008; Xiao et al. 2009). Seed availability is the prerequisite for seedling establishment on tidal flats and hydrodynamic-induced seed removal from the tidal flat surface is a major source of seed loss (Groenendijk 1986; Marion and Orth 2012; Zhu et al. 2014). Hence, we first determined the response of surface seed retention to increasing wave actions by conducting large-scale experiments in field locations with varying wave forcing in a NW Delta, the Scheldt estuary (Fig. 2a). Based on this relationship, we next develop a spatial model to assess the consequences of SLR-intensified wave forcing for seed-based vegetation recoverability.

Materials and methods

Quantifying the response of seed retention to varying wave forcing on tidal flats

Study sites and species

The Scheldt estuary is a macrotidal estuary situated near the border between the Netherlands and Belgium. The mean tidal range increases from 3.8 m near the mouth of the estuary to > 5.0 m upstream of the border (Baeyens et al. 1998). It was originally composed of two aligned and interconnected waterbodies called Westerschelde and Oosterschelde. Due to land reclamation in 1860s, the Oosterschelde was progressively separated from the Westerschelde. The pioneer saltmarsh vegetation in the meso- and polyhaline (> 5 ppt) part of the estuary consists mainly of the perennial common cordgrass (*Spartina anglica*), which was introduced to the Scheldt estuary in the 1920s (Groenendijk 1986; van der Wal et al. 2008).

Cordgrass can produce a large amount of seeds, although there is high variability between years and locations (Gray et al. 1991; Xiao et al. 2009; Strong and Ayres 2013). Because of the short (< 1 yr) seed longevity (Wolters and Bakker 2002; Xiao et al. 2009), seedling establishment of cordgrass on tidal flats requires annually built seed banks as a result of seed delivery from the marsh by the tide (Huiskes et al. 1995; Zhu et al. 2014). Although the minimal period that such transient seed banks need to persist is short, i.e., the period between when seeds become available (autumn) and seedlings start to emerge (spring), the persistence during this short period is vital for the occurrence of seedling recruitment (Groenendijk 1986; Zhu et al. 2014). Seed dislodgement by waves and associated sediment erosion is a major source of seed loss from the tidal flat; seeds are especially vulnerable when they are on the surface (Groenendijk 1986; Zhu et al. 2014).

Quantifying seed retention under varying wave conditions

To quantify the relationship between surface seed retention and wave forcing, we selected eight field locations (tidal flats near a marsh) in the Scheldt estuary with varying water depth (Fig. 2a; Table 1), including both relatively wind sheltered and exposed sites (Callaghan et al. 2010; Suykerbuyk et al. 2016). The study locations include seven mudflats near the marsh in the Scheldt estuary (Fig. 2a) with different wind exposure (Callaghan et al. 2010; Suykerbuyk et al. 2016); The elevation of the experimental area was about 90 cm above NAP (i.e., Dutch ordinance level, close to mean sea level) for most field sites, while a higher elevation (175 cm NAP) was chosen for two Westerschelde sites: ZG and BA where saltmarshes are less deep. At ZG, we included an additional location with a lower elevation (ca. 90 cm NAP).

Our experiments and measurements were implemented during the relatively storm-free period, April–July (T0–T4, Supporting Information Table S1) to obtain a range of wave conditions including both small and large waves. At each location, we quantified the retention of surface seeds by seed sowing and recovery experiments. We conducted three trials at each site with a duration of 4 weeks (trial 1: T0–T1; trial2: T1–T2) and 2 weeks (trial 3: T3–T4). In each trial, five 20 × 20 cm quadrats were laid in a row at 1 m intervals. Within each quadrat, 50 cordgrass seeds were randomly sowed on the sediment surface. These quadrats were positioned along a 6 m-long string (marked every 1 m) with each end fixed at a PVC tube. The sowed seeds were first sterilized by freezing them in a −20°C freezer for 2 weeks to prevent seed loss due to germination (Zhu et al. 2016). These seeds were then dyed with Rose Bengal to be distinguished from the ambient seeds and were waterlogged to mimic the naturally settled cordgrass seeds (Zhu et al. 2014).

Upon recovery, sediment bulks (each 40 × 40 × 5 cm, length × width × depth) were excavated after relocation of the quadrates using the same string. There was no seed visible on the surface when recovered. We sampled the top 5 cm to recover

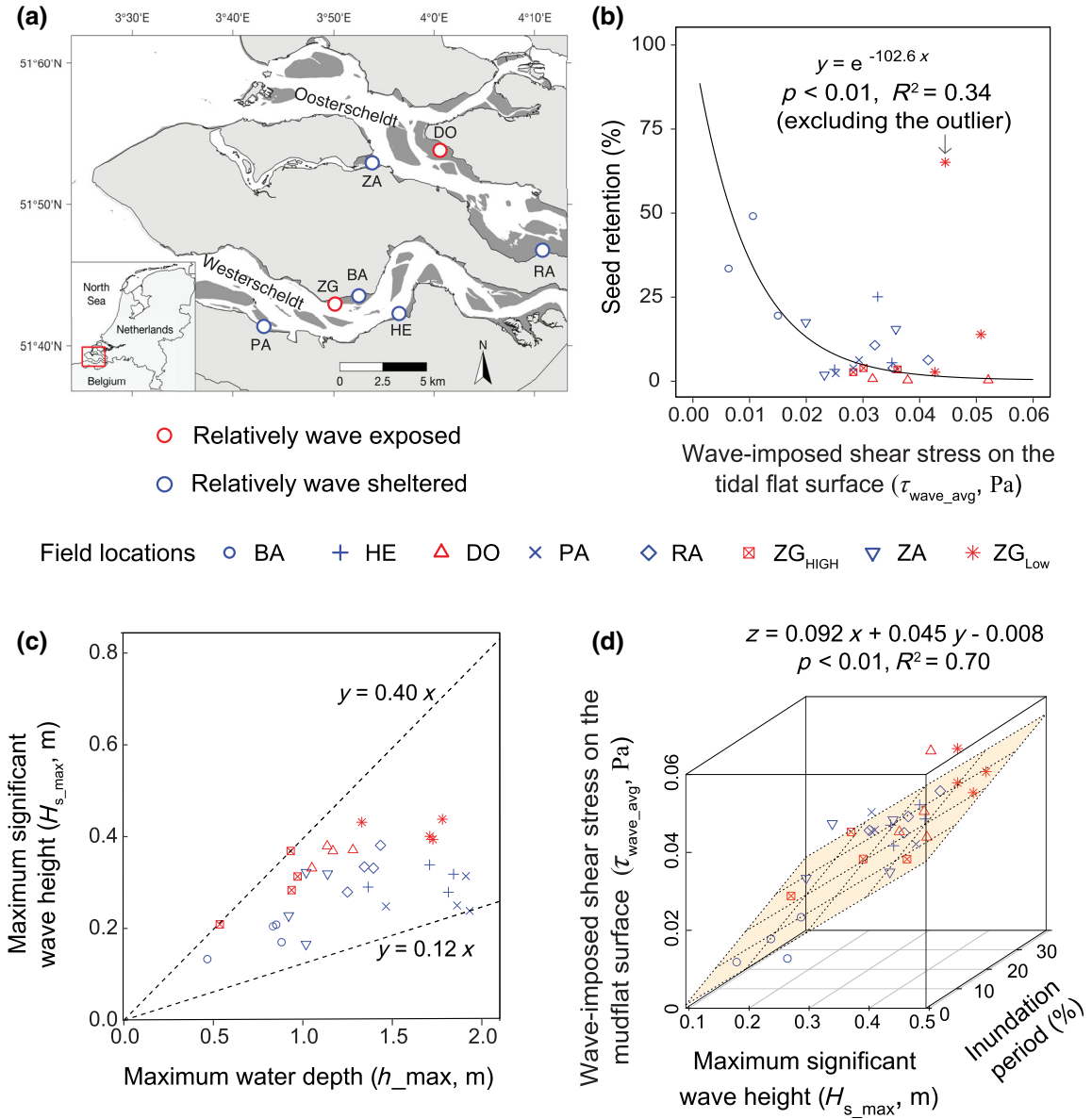

Fig. 2. (**a**) Geographic locations of the selected field sites; sites marked in red are relatively wave-exposed and those in blue are relatively sheltered. Site ZG includes two locations of different intertidal elevations: ZG_{HIGH} and ZG_{LOW}. Detailed site characteristics are shown in Supporting Information Table 1. (**b**) Surface seeds retention declined exponentially with time-averaged wave-induced bed shear stress (τ_{wave_avg}). This relation was significant (Pearson's correlation, $p < 0.01$) when excluding the only outlier observed at ZG_{LOW}. (**c**) Observed relationship between maximum significant wave height (H_{s_max}) and maximum water depth ($h_{\_max}$). (**d**) Time-averaged wave-induced bed shear stress (τ_{wave_avg}) correlates positively with maximum significant wave height and inundation period (linear model, $p < 0.001$).

the seeds that may have been buried. The recovered area was chosen to be twice as big as the seed-deployment area, to account for the seeds that might have merely moved to the close vicinity. Seeds not recovered within this area were regarded as "lost." The retrieved sediment was transported back to the lab and sieved through a 0.1 cm sieve, to quantify the remaining seeds. Seed retention (%) during each trial period was calculated as recovered/deployed and averaged among the five replicates at each location.

Quantifying wave forcing in relation to seed retention

The wave forcing and tidal level of each location was measured in 2013 during T0–T4 (Supporting Information Table S1), using pressure sensors (OSSI-010-003C; Ocean Sensor Systems) deployed in the experiment zone. Every wave gauge was mounted on a pole inserted into the soil about 1 m deep. Each sensor was approximately 5 cm above the tidal flat surface. The measuring interval and period were 15 min and 7 min, respectively. The wave analysis was based on pressure fluctuations, measured with

Table 1. Characteristics of field locations.

Field locations		Wind exposure	Elevation (cm NAP)	Maximum water depth (m)	Medium grain size (μm)
Oosterschelde	DO	Exposed	90	1.3	159.8
	RA	Sheltered	92	1.4	98.1
	ZA	Sheltered	85	1.1	96.3
Westerschelde	ZG_{LOW}	Exposed	89	1.8	72.0
	ZG_{HIGH}	Exposed	175	1.0	50.2
	BA	Sheltered	175	0.9	23.6
	HE	Sheltered	102	1.8	109.6
	PA	Sheltered	82	1.9	76.0

a frequency of 5 Hz. The recorded pressure readings were converted to water level fluctuations, which were then corrected by removing erroneous spikes, shifts, corrupted bursts, and low frequency tidal components (Callaghan et al. 2010; Christianen et al. 2013). From the detrended data, wave parameters, including significant wave height (H_s) and peak wave period (T_p), were calculated based on the linear wave theory (Tucker and Pitt 2001).

Wave-induced shear stress (τ_{wave}, Pa) on the sediment surface is a relevant measure for the hydrodynamic energy in relation with sediment motion (Callaghan et al. 2010), making it a good proxy for the wave forcing that dislodge seeds on the surface. τ_{wave} is calculated as follows (van Rijn 1993):

$$\tau_{wave} = \frac{1}{4}\rho_w f_w \hat{U}_\delta^2$$

where ρ_w is the seawater density (kg m^{-3}); $\hat{U}_\delta$ is near-bed orbital velocity, calculated as:

$$\hat{U}_\delta = \frac{\pi H}{T \sinh(kh)}$$

in which H is wave height (m), T is wave period (s), k is wave number (m^{-1}), calculated by solving $(2\pi/T)^2 = gk\tanh(kh)$ (Swart 1977), and h is water depth (m). In practice, significant wave height H_s and peak wave period T_p are used as H and T in the formulae.

The wave friction coefficient f_w is determined by the following equation (Swart 1977):

$$f_w = \min\left\{\exp\left[-6 + 5.2\left(\frac{\hat{A}_\delta}{2.5\, d_{50}}\right)^{-0.19}\right], 0.3\right\}$$

where the peak orbital excursion $\hat{A}_\delta$ is expressed as $\hat{A}_\delta = \frac{H}{2\sinh(kh)}$, d_{50} is median grain size of the bed sediment (m).

A breaking-wave check was carried out before the τ_{wave} calculation, as the theory mentioned above is applied to nonbreaking waves. In our cases, wave heights over water depths (H_s/h) were all < 0.78, indicating local nonbreaking condition (Kaminsky and Kraus 1993).

For each location, we determined the time-averaged wave-imposed shear stress (τ_{wave_avg}) on the tidal flat surface to measure the overall wave disturbance to the surface seeds. τ_{wave_avg} was determined for four monitoring period T0–T1, T1–T2, T2–T3, and T3–T4, respectively (Supporting Information Table S1). For each period, we also determined maximum significant wave height (H_{s_max}), water depth ($h_{\_max}$), and inundation frequency.

Measurement of bed level change

Additionally, the elevation in the experimental zone of each location was monitored monthly using a 3D Laser scanner (RIEGL VZ-400) to detect the patterns of bed level change of each location. All the scans were georeferenced with the Riscan program that came with the scanner. The scans were clipped to the experiment zone. The resulting points were exported to an LAS-file that was later imported to ArcGis10. For each 5 × 5 cm, the maximum value is used to produce a raster. To partly fill the holes in the raster, the maximum value for each 20 × 20 cm was also adopted. The two rasters were mosaicked, 5 cm on top. For each location, 20 random points from an undisturbed area (ca. 75 × 75 cm) in each plot and the undisturbed area in between plots were selected, respectively, to calculate the mean elevation at each time point. The scanning was conducted at T0, T1, T2, and T5 (Supporting Information Table S1). Due to the instrument failure, elevation values were not available at T2 for DO, RA, and ZA.

Statistics

Data from all field locations were pooled together for statistics. We used Pearson's correlation to analyze the relationship between seed retention and τ_{wave_avg}. Prior to the analysis, data normality was checked through Shapiro–Wilk tests. The seed retention was square root-transformed to satisfy the requirement of data normality. After a significant correlation between seed retention and τ_{wave_avg} was found, we applied different types of curve fits (including both linear and nonlinear) to find a regression equation that can best explain the relationship between these two variables. All the statistical analyses were done in

R (http://www.R-project.org), applying a significance level of $\alpha = 0.05$.

Modeling the impacts of intensified wave forcing on revegetation of tidal flats

We developed a cellular automation-based model to assess the consequences of SLR-intensified wave forcing for seed-based marsh recoverability on neighboring tidal flats. The model domain consists of a matrix of 1000 × 1000 cells, which represent a landscape of 100 × 100 m with each cell 0.1 × 0.1 m. In this model, revegetation of tidal flats starts with seedling recruitment, which serves as nuclei for subsequent vegetative growth (Fig. 1d–f). For each cell, there are three possible states: bare state, seedling state, or vegetated state. The model starts with a landscape consisted of bare cells. A bare cell first shifts to a seedling cell when seedling recruitment occurs, and later becomes a vegetated cell at the end of each year (time step). A bare cell can also directly change into a vegetated cell by vegetative growth when there are vegetated cells in the neighborhood.

The number of cells that transfer from the "bare" state to "seedling" state increases with seedling density (number per m^2). Seedling density is set to decrease with increasing distance to the marsh edge with its peak occurring near the marsh edge, complying with observed patterns in the field (Xiao et al. 2010; Zhu et al. 2012). Peak seedling density (D_{peak}) is determined by two parameters: (1) the wave-imposed shear stress on the tidal flat surface (τ_{wave_avg}, Pa), the primary factor limiting seedling density by minimizing seed retention on tidal flats; and (2) a seedling abundance coefficient (Sc), reflecting the lumped effects of all factors other than waves on seedling recruitment, such as seed availability, seed germination, and seedling-mortality caused by various factors, e.g., sediment erosion (Bouma et al. 2016; Cao et al. 2018), bioturbation (van Wesenbeeck et al. 2007), herbivory (Paramor and Hughes 2004; Zhu et al. 2016), and so on. A lower value of Sc means stronger inhibition on seedling recruitment from these factors and vice versa.

D_{peak} is calculated by the following equation:

$$D_{peak} = \mathrm{Sc}^* e^{-102.6^* \tau_{wave\_avg}}$$

Seedling density at a given distance is calculated as:

$$D_s = D_{peak}^* \mathrm{Ks}/(\mathrm{Ks} + \mathrm{ds})$$

where ds (an integer between 1 and 1000) is the distance to the marsh edge and Ks is the half saturation constant for ds. Since the decay rate of seed delivery and seedling survival with increasing distance to the marsh edge can be highly site-specific, we made Ks a random integer between 10 (1 m) and 250 (25 m). We applied this maximum value based on the field data from a Chinese marsh with the ever-reported fastest cordgrass expansion by seedling recruitment (Xiao et al. 2010; Zhu et al. 2012).

The number of seedling cells at a given distance is determined as:

$$n_s = \min(D_s^* n^* A, n)$$

where n is the number of cells at that distance and A is the area of each cell (i.e., 0.01 m^2). The positions of the seedling cells at a given distance were randomly determined.

To account for stochastic disasters such as severe storms that may wipe out all the seeds or established seedlings, the model randomly decides whether a given year is a bad year. When it is a "bad year," seedling cells turn back to bare cells at the end of the year, whereas seedling cells become vegetated cells at the end of each good year.

The transition probability from a bare cell to a vegetated cell by clonal growth is determined by the number of neighboring vegetated cells. The neighborhood size is determined by clonal growth rate. Since clonal growth rate of cordgrass was found to be highly variable and usually < 2 m (i.e., 20 cells) per year (Gray et al. 1991; Xiao et al. 2010; Zhu et al. 2012), we adopted a random integer between 1 and 20 for clonal growth rate (cells yr^{-1}) for each time step.

We conducted numeric experiments by varying both the values of wave-imposed shear stress on the tidal flat surface τ_{wave_avg} and the seedling abundance coefficient Sc. For τ_{wave_avg}, we applied a wide range of values from 0.01 to 0.08 Pa (based on field observation, Fig. 2d) with an interval of 0.0025 Pa, and we adopted three distinct values (0.01, 0.1, and 1) for Sc to reproduce seedling densities that cover the natural range for cordgrass seedlings observed in the field (Gray et al. 1991; Xiao et al. 2010; Zhu et al. 2012; Liu et al. 2017). For each combination of τ_{wave_avg} and Sc, we first sort out the scenarios when seed colonization is completely disabled. Where seedling establishment is possible, we run the model 100 times, and for each run, we determined the recovery time, i.e., the number of years it takes to recover the given 100 × 100 m landscape. The landscape is considered as "recovered" when 90% of the cells become vegetated. After these initial runs, we added three sets of scenarios to detect the sensitivity of recovery time to small increments of wave heights. For each set of scenario, we raised τ_{wave_avg} by 0.001 Pa, 0.002 Pa, and 0.003 Pa, respectively, which corresponds to approximately 1 m, 2 m, and 3 cm rise of maximum significant wave height, respectively, according to the empirical relationship derived from our field measurements (Fig. 2d). We ran each scenario 100 times and determined the recovery time, which was then averaged and compared to the initial recovery time to detect how raised wave heights cause changes in marsh vegetation recoverability on tidal flats.

Results

Effects of increasing wave disturbance on seed retention on tidal flats

The field results showed that the persistence of the seeds on the tidal flat surface decayed exponentially with increasing wave disturbance (Fig. 2b), measured as the time-averaged

shear stress that the waves imposed on the tidal flat surface (τ_{wave_avg}). This relation is significant (Pearson's correlation, $p < 0.01$) when excluding the only outlier (i.e., the extremely high value) observed at ZG_{LOW} (Fig. 2b). ZG_{LOW} is the sole location characterized by continuously fast sediment accretion (ca. 1.2 mm d^{-1}, Supporting Information Fig. S1), which most likely result from the dumping of dredged sediment near this location (Sistermans and Nieuwenhuis 2019). This may explain the outlier, as fast sediment accretion might occasionally offer the seeds a window of opportunity to get sufficiently buried to escape subsequent wave disturbance on surface seed. Such burial-scenario is, however, expected to be rare, given the rarity of fast accretion in autumn, winter, and early spring (Andersen et al. 2006; Yang et al. 2008; Zhu et al. 2012; Hu et al. 2017), during which cordgrass seeds are dispersed (Huiskes et al. 1995; Xiao et al. 2009). When excluding all the data points ($n = 3$ for ZG_{LOW} and $n = 1$ for BA) associated with fast sediment accretion (> 1 mm d^{-1}, Supporting Information Fig. S1), the relationship between seed retention and τ_{wave_avg} remains significant (Pearson's correlation, $p < 0.01$, Supporting Information Fig. S2) with a comparable declining trend as shown in Fig. 2b.

Field measurements reveal a clear positive effect of water depth on wave strength, supporting the assumption that SLR-increased water depth on tidal flats intensifies wave forcing. Increased water depth allows higher maximum significant wave heights (Fig. 2c), which is proportional to mean significant wave heights (Supporting Information Fig. S3). Increased maximum significant wave heights, plus a longer inundation period due to raised water depths, results in stronger shear stress wave imposed on the tidal flat surface (Fig. 2d). For a given water depth, the relatively wave exposed sites have higher wave heights than the relatively wave sheltered sites (Fig. 2c), indicating that SLR impacts on wave forcing may be amplified if climate change leads to stronger or more frequent winds toward the coasts.

Modeling the impacts of intensified wave forcing on marsh revegetation

The model reveals the same vegetation expansion dynamics as observed in the field: seedling establishment yields satellite clumps, which then extend laterally and eventually merge into continuous meadows through clonal growth (Fig. 3). The number of established seedlings thus strongly controls the speed of vegetation expansion on the tidal flats (Fig. 3). Hence, mean revegetation rate increases nonlinearly with increasing peak seedling density, but it becomes more or less constant once the peak seedling density (number per m^2) becomes higher than 10 (Fig. 4a). Peak seedling density declines nonlinearly with time-averaged wave-induced bed shear stress (τ_{wave_avg}), with its magnitude regulated by the seedling abundance coefficient (Fig. 4b).

Generally, under nominal conditions, our model produced comparable revegetation rates as observed in the field. For example, a 100 m long (cross-shore) tidal flat was predicted to be

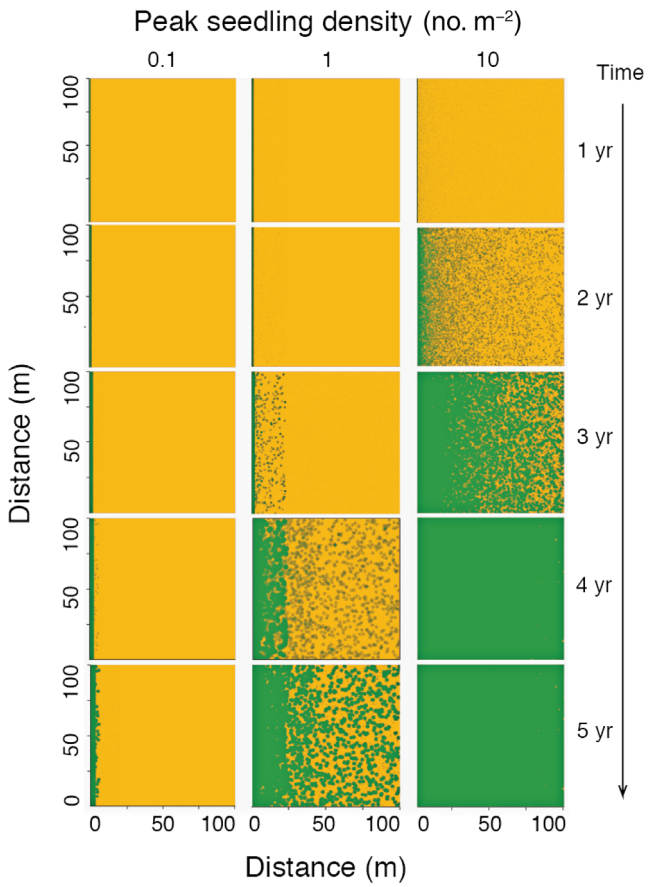

Fig. 3. Temporal dynamics of vegetation expansion/recovery on tidal flats under three different scenarios of peak seedling density. For each scenario, one typical example of vegetation expansion process within 5 yr was shown. The vegetation was marked in green with the bare mudflat shown in brown.

vegetated with an average expansion rate of 28 m yr^{-1} for a peak seedling density of about 6 no. m^{-2} (Fig. 4a), which parallels the observed rapid cordgrass expansion in a Chinese marsh with comparable seedling densities: 25 m in 2009 (Xiao et al. 2010) and 39 m in 2010 (Zhu et al. 2012). Moreover, field observations in saltmarshes in East Asia (Xiao et al. 2010; Zhu et al. 2012; Liu et al. 2017; Cao et al. 2018), NW Europe (Gray et al. 1991; Nehring and Hesse 2008; Bouma et al. 2016), and the Pacific coast of U.S. (Ayres et al. 2004; Strong and Ayres 2013) confirm our model predictions that seedling recruitment allows for much faster vegetation establishment than what would be observed when clonal growth from the existing marsh edge is the only driving process (Fig. 4a).

The model results (Fig. 5a) clearly show that vegetation recovery time grows nonlinearly with increasing wave-imposed shear stress on the tidal flat surface (τ_{wave_avg}) until seed colonization is completely disabled. The sensitivity of the recovery rate to rising τ_{wave_avg} decreases with increased value of seedling abundance coefficient (i.e., reduced negative effects from other stressors), while it increases with declined seedling density. For instance, increased τ_{wave_avg} does not affect recovery rate much when peak

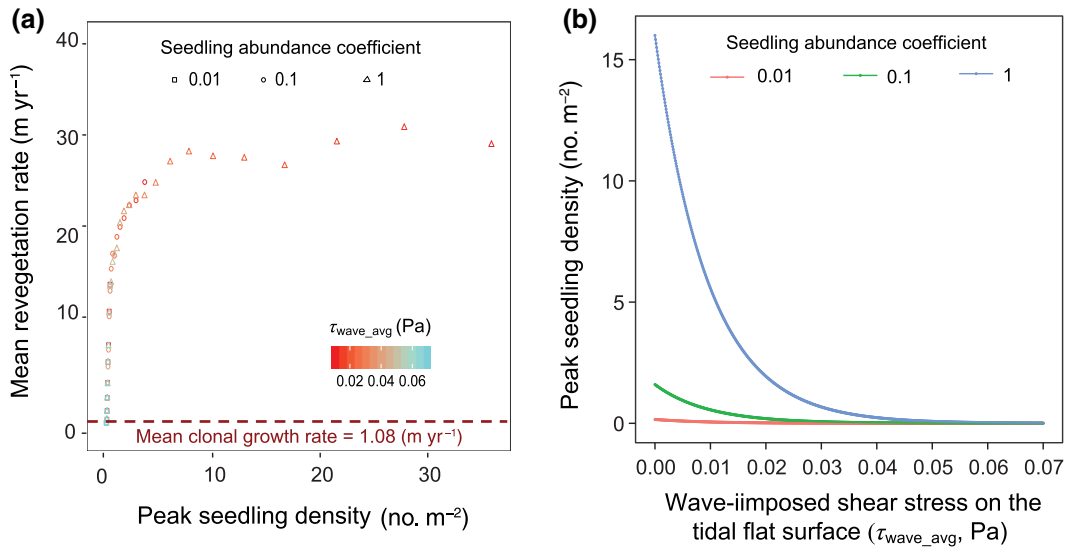

Fig. 4. (**a**) In the model, mean revegetation rate (m yr^{-1}) increases nonlinearly with peak seedling density. Revegetation is generally much faster when seed colonization is enabled than when revegetation is achieved by only clonal growth from the existing marsh edge. Time-averaged wave-induced bed shear stress (τ_{wave_avg}) affects the revegetation rate by modifying peak seedling density. (**b**) Peak seedling density declined nonlinearly with τ_{wave_avg}, with its magnitude regulated by seedling abundance coefficient, a parameter that reflects the lumped effects of all factors other than waves on seedling recruitment.

seedling density is higher than 0.4 no. m^{-2}, whereas it greatly slows down and eventually disables seed-based revegetation when peak seedling density is between 0 and 0.4 no. m^{-2} (Fig. 5a).

Further analyses reveal that a small increase of wave height on tidal flats due to SLR-increased water depth can considerably lengthen marsh recovery time, especially when the initial recovery is already slow (Fig. 5b). For instance, with a low

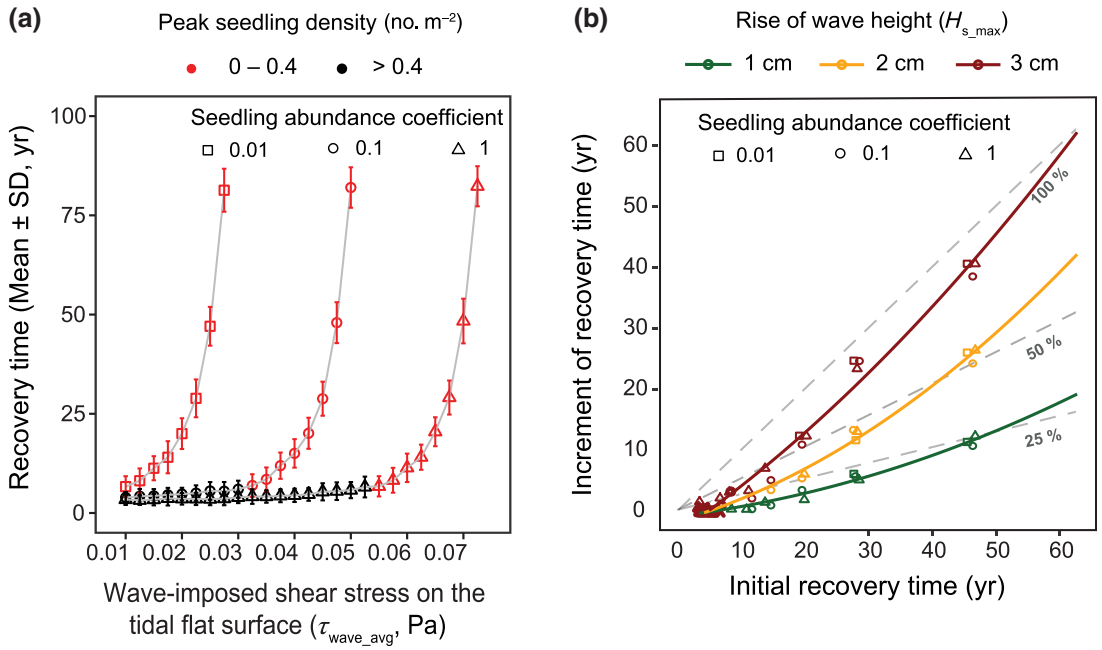

Fig. 5. (**a**) Modeled marsh recovery time (mean ± SD, $n = 100$) grows rapidly with increasing wave-imposed shear stress on the tidal flat near the marsh edge (τ_{wave_avg}, Pa) when the peak seedling density (number per m^2) is low (0–0.4), whereas the recovery time did not change much with a high (> 0.4) peak seeding density. The sensitivity of recovery time to τ_{wave_avg} increases with decreased value of seedling abundance coefficient, i.e., stronger negative effects from other stressors. (**b**) The response of recovery time lengthening to small increases (1, 2, and 3 cm) of maximum significant wave height (H_{s_max}) due to the deeper water conditions on the tidal flat as result of SLR, in relation to the initial recovery time. The data points include both scenarios of peak seedling density (number per m^2), i.e., "0–0.4" and "> 0.4." Each curve fit was done with a quadratic function $y = a^*x^2$, which explained best the observed increasing trend. The three dashed reference lines represent the conditions when the increment of recovery time is 25%, 50%, and 100% of the initial recovery time, respectively.

initial recoverability (recovery time = 47 yr), a 3 cm rise of maximum significant wave height (H_{s_max}) nearly doubles the recovery time and even only a 1 cm increase of H_{s_max} lengthens the recovery time by approximately 25% (Fig. 5b). In the field locations used in this study, 1 cm rise of maximum significant wave height can be achieved by an increase of maximum water depth between 2.5 and 8.3 cm, depending on wave exposure (Fig. 2c).

Discussion

The current study highlights that saltmarshes are more vulnerable to SLR than previously considered. Our results reveal high sensitivity of seed-based revegetation of bare tidal flats to intensified wave forcing that nonlinearly lengthens the vegetation recovery time. A small increase of water depth on the tidal flat resulting from SLR is able to cause a major decline in lateral marsh recoverability (i.e., marsh resilience to lateral erosion) by lowering seed persistence. Hence, revegetation of tidal flats next to the marsh edge forms an Achilles' heel of saltmarsh resilience to SLR in systems where vegetation recovery typically starts from seeds, as seen in many meso- and macrotidal systems (Gray et al. 1991; Temmerman et al. 2007; Strong and Ayres 2013; Liu et al. 2017). While recent literature highlights that the risk of saltmarsh drowning in response to SLR has been overstated as marshes are able to adapt when sediment availability is sufficient (Kirwan et al. 2016), the current study demonstrates that SLR can significantly weaken marsh resilience at the seaward boundary by hampering vegetation recovery from seeds at the seaward edge of an eroding marsh.

In addition to the primary findings, the results also suggest that SLR impacts on seed-based marsh recovery may be magnified by other stressors such as bioturbation (van Wesenbeeck et al. 2007) and herbivory (Paramor and Hughes 2004; Zhu et al. 2016) that can inhibit seedling recruitment. Enhanced negative effects (i.e., lower seedling abundance coefficient) from such stressors increase the sensitivity of the marsh recovery process to changing wave forcing (Fig. 5a). In addition, despite the revealed strong impacts of waves on seed-based revegetation, the present assessment is likely to be underestimated, as we only looked at seed removal and did not consider the negative effects of wave disturbance on seedling survival (Bouma et al. 2016). In reality, seed-based vegetation recovery of cordgrass on neighboring tidal flats may be more susceptible to SLR increased wave forcing than what we showed in the model.

Given raised lateral marsh erosion risks under SLR as shown in earlier studies (Mariotti and Fagherazzi 2010; Leonardi et al. 2016; Wang et al. 2017), declined vegetation recoverability on adjacent tidal flats may over time result in a near-irreversible lateral marsh collapse, due to increased wave exposure resulting from raised water depths (Mariotti and Fagherazzi 2010; Arns et al. 2017, this study). Although vertical marsh adaptability eases the risk of coastal squeeze (Pontee 2013), i.e., reduced marsh width due to SLR-induced drowning along with prevented landward migration by seawalls (or otherwise called dikes, levees etc.), our study highlights that marshes in front of seawalls still can suffer significant habitat loss due to declined lateral marsh recoverability to lateral erosion. This can impair the value of key ecosystem services of saltmarshes such as flood protection which depends critically on ecosystem size (Bouma et al. 2014), especially for marshes that have already declined in area due to land reclamation (Kirwan and Megonigal 2013).

This article underscores the importance of maintaining a cascade protection of ecosystems for supporting resilient coasts. Habitats at lower tidal elevations (i.e., the bare tidal flat) that do not make a direct contribution for flood defense can influence the resilience and long-term persistence of ecosystems at higher tidal elevations (e.g., saltmarshes) that directly protect the coast against flooding (Mariotti and Fagherazzi 2013; Bouma et al. 2014). Maintaining sustainable nature-based coastal defenses by saltmarshes in the face of SLR thus entails not only an adaptable marsh platform, but also ensuring protection of the neighboring tidal flats that allows for resilient marshes. Hence, management policies should enforce a cascade of protection: maintain well-elevated or wave-protecting tidal flats to sustain resilient marshes and thus safer coasts. This may be achieved by supply of dredging materials (Mendelssohn and Kuhn 2003; Temmerman et al. 2013) to reach a sufficiently high accretion rate that allows the tidal flat to adapt to SLR or by restoring shellfish reef ecosystems that limit wave formation on the tidal flat (Scyphers et al. 2011; Temmerman et al. 2013).

The present research underpins recent suggestions to manage ecosystem connectivity in order to preserve coastal ecosystems (Gillis et al. 2014, 2017). Moreover, we demonstrate how such an approach becomes increasingly important in the face of global change. Beyond saltmarshes and adjacent tidal flats, other connected ecosystems may also display a cascade of vulnerability to environmental changes. For instance, in tropical coastal ecosystems, habitat losses of wave-damping coral reefs or seagrass beds due to climate change or human disturbances risk weakened stability of the neighboring mangrove forests (Gillis et al. 2014, 2017). Similarly, the resilience of upland Amazon forests is likely to be impaired by the adjacent floodplains, which are more prone to the shift into a fire-dominated savanna state when the Amazon region becomes drier under climate change (Flores et al. 2017). Hence, we argue that the cascading protection strategy may be commonly needed to enhance the overall resilience of important landscapes or seascapes, constituted by spatially and functionally connected ecosystems, to the changing environment.

To conclude, we reveal saltmarsh recovery on the neighboring tidal flat habitats as an unrecognized Achilles' heel of saltmarsh resilience to SLR. The present findings are highly relevant for a more comprehensive assessment of marsh susceptibility to SLR and more accurate predictions of long-term dynamics of marshes where seeds play a critical role in vegetation recruitment. While coastal wetlands, such as saltmarshes,

are increasingly proposed to act as climate-change buffers to enhance the resilience of coastal communities (Duarte et al. 2013; Temmerman et al. 2013; Bouma et al. 2014), our study suggests that human intervention would be duly needed to improve the resilience of these buffering ecosystems as well as their protecting neighbors to warrant a sustainable, nature-based, coastal adaptation to global climate change.

Data availability statement

The code of the model and the field data of waves and seed retention that support the findings of this study are available in 4TU.ResearchData: https://doi.org/10.4121/uuid:c160edca-6234-439b-8600-5c6f7d81b46e.

References

Allen, J. R. 2000. Morphodynamics of Holocene salt marshes: A review sketch from the Atlantic and Southern North Sea coasts of Europe. Quat. Sci. Rev. **19**: 1155–1231. doi:10.1016/S0277-3791(99)00034-7.

Allison, S. K. 1995. Recovery from small-scale anthropogenic disturbances by northern California salt marsh plant assemblages. Ecol. Appl. **5**: 693–702. doi:10.2307/1941978.

Andersen, T. J., M. Pejrup, and A. A. Nielsen. 2006. Long-term and high-resolution measurements of bed level changes in a temperate, microtidal coastal lagoon. Mar. Geol. **226**: 115–125. doi:10.1016/j.margeo.2005.09.016.

Angelini, C., and B. R. Silliman. 2012. Patch size-dependent community recovery after massive disturbance. Ecology **93**: 101–110. doi:10.1890/11-0557.1.

Arns, A., S. Dangendorf, J. Jensen, S. Talke, J. Bender, and C. Pattiaratchi. 2017. Sea-level rise induced amplification of coastal protection design heights. Sci. Rep. **7**: 40171. doi:10.1038/srep40171.

Ayres, D. R., D. L. Smith, K. Zaremba, S. Klohr, and D. R. Strong. 2004. Spread of exotic cordgrasses and hybrids (*Spartina sp.*) in the tidal marshes of San Francisco Bay, California, USA. Biol. Invasions **6**: 221–231. doi:10.1023/B:BINV.0000022140.07404.b7.

Ayres, D. R., K. Zaremba, C. M. Sloop, and D. R. Strong. 2008. Sexual reproduction of cordgrass hybrids (*Spartina foliosa* x alterniflora) invading tidal marshes in San Francisco Bay. Divers. Distrib. **14**: 187–195. doi:10.1111/j.1472-4642.2007.00414.x

Baeyens, W., B. van Eck, C. Lambert, R. Wollast, and L. Goeyens. 1998. General description of the Scheldt estuary. Hydrobiologia **366**: 1–14. doi:10.1023/A:1003164009031.

Balke, T., E. L. Webb, E. van den Elzen, D. Galli, P. M. J. Herman, and T. J. Bouma. 2013. Seedling establishment in a dynamic sedimentary environment: A conceptual framework using mangroves. J. Appl. Ecol. **50**: 740–747. doi:10.1111/1365-2664.12067.

Barbier, E. B., S. D. Hacker, C. Kennedy, E. W. Koch, A. C. Stier, and B. R. Silliman. 2011. The value of estuarine and coastal ecosystem services. Ecol. Monogr. **81**: 169–193. doi:10.1890/10-1510.1.

Bouma, T. J., and others. 2009. Effects of shoot stiffness, shoot size and current velocity on scouring sediment from around seedlings and propagules. Mar. Ecol. Prog. Ser. **388**: 293–297. doi:10.3354/meps08130.

Bouma, T. J., and others. 2014. Identifying knowledge gaps hampering application of intertidal habitats in coastal protection: Opportunities & steps to take. Coast. Eng. **87**: 147–157. doi:10.1016/j.coastaleng.2013.11.014.

Bouma, T. J., and others. 2016. Short-term mudflat dynamics drive long-term cyclic salt marsh dynamics. Limnol. Oceanogr. **61**: 2261–2275. doi:10.1002/lno.10374.

Callaghan, D. P., T. J. Bouma, P. Klaassen, D. van der Wal, M. J. F. Stive, and P. M. J. Herman. 2010. Hydrodynamic forcing on salt-marsh development: Distinguishing the relative importance of waves and tidal flows. Estuar. Coast. Shelf Sci. **89**: 73–88. doi:10.1016/j.ecss.2010.05.013.

Cao, H., Z. Zhu, T. Balke, L. Zhang, and T. J. Bouma. 2018. Effects of sediment disturbance regimes on *Spartina* seedling establishment: Implications for salt marsh creation and restoration. Limnol. Oceanogr. **63**: 647–659. doi:10.1002/lno.10657.

Chauhan, P. P. S. 2009. Autocyclic erosion in tidal marshes. Geomorphology **110**: 45–57. doi:10.1016/j.geomorph.2009.03.016.

Christianen, M. J. A., and others. 2013. Low-canopy seagrass beds still provide important coastal protection services. PLoS One **8**: e62413. doi:10.1371/journal.pone.0062413.

Costanza, R., and others. 1997. The value of the world's ecosystem services and natural capital. Nature **387**: 253–260. doi:10.1038/387253a0.

Deegan, L. A., and others. 2012. Coastal eutrophication as a driver of salt marsh loss. Nature **490**: 388–392. doi:10.1038/nature11533.

Duarte, C. M., I. J. Losada, I. E. Hendriks, I. Mazarrasa, and N. Marbà. 2013. The role of coastal plant communities for climate change mitigation and adaptation. Nat. Clim. Chang. **3**: 961–968. doi:10.1038/nclimate1970.

Flores, B. M., and others. 2017. Floodplains as an Achilles' heel of Amazonian forest resilience. Proc. Natl. Acad. Sci. USA **114**: 4442–4446. doi:10.1073/pnas.1617988114.

Friess, D. A., and others. 2012. Are all intertidal wetlands naturally created equal? Bottlenecks, thresholds and knowledge gaps to mangrove and saltmarsh ecosystems. Biol. Rev. **87**: 346–366. doi:10.1111/j.1469-185X.2011.00198.x.

Gillis, L. G., and others. 2014. Potential for landscape-scale positive interactions among tropical marine ecosystems: A review. Mar. Ecol. Prog. Ser. **503**: 289–303. doi:10.3354/meps10716.

Gillis, L. G., C. Jones, A. Ziegler, D. van der Wal, A. Breckwoldt, and T. Bouma. 2017. Opportunities for protecting and restoring tropical coastal ecosystems by utilizing a physical connectivity approach. Front. Mar. Sci. **4**: 374. doi:10.3389/fmars.2017.00374.

Gray, A. J., D. F. Marshall, and A. F. Raybould. 1991. A century of evolution in *Spartina anglica*. Adv. Ecol. Res. **21**: 1–62. doi:10.1016/s0065-2504(08)60096-3.

Groenendijk, A. M. 1986. Establishment of a *Spartina-anglica* population on a tidal mudflat - a field experiment. J. Environ. Manage. **22**: 1–12.

Holdredge, C., M. D. Bertness, and A. H. Altieri. 2009. Role of crab herbivory in die-off of New England salt marshes. Conserv. Biol. **23**: 672–679. doi:10.1111/j.1523-1739.2008.01137.x.

Hu, Z., P. Yao, D. van der Wal, and T. J. Bouma. 2017. Patterns and drivers of daily bed-level dynamics on two tidal flats with contrasting wave exposure. Sci. Rep. **7**: 7088. doi:10.1038/s41598-017-07515-y.

Hughes, Z. J., D. M. FitzGerald, C. A. Wilson, S. C. Pennings, K. Więski, and A. Mahadevan. 2009. Rapid headward erosion of marsh creeks in response to relative sea level rise. Geophys. Res. Lett. **36**: L03602. doi:10.1029/2008GL036000.

Huiskes, A. H. L., B. P. Koutstaal, P. M. J. Herman, W. G. Beeftink, M. M. Markusse, and W. D. Munck. 1995. Seed dispersal of halophytes in tidal salt marshes. J. Ecol. **83**: 559–567. doi:10.2307/2261624.

Kaminsky, G. M., and N. C. Kraus. 1993. Evaluation of depth-limited wave breaking criteria, p. 180–193. *In* Magoon, O. T. and Hemsley, J. M. (eds.), Proceedings of 2nd International Symposium on Ocean Wave Measurement and Analysis, Waves 93 (ASCE, New York).

Kirwan, M. L., and J. P. Megonigal. 2013. Tidal wetland stability in the face of human impacts and sea-level rise. Nature **504**: 53–60. doi:10.1038/nature12856.

Kirwan, M. L., S. Temmerman, E. E. Skeehan, G. R. Guntenspergen, and S. Fagherazzi. 2016. Overestimation of marsh vulnerability to sea level rise. Nat. Clim. Chang. **6**: 253–260. doi:10.1038/nclimate2909.

Leonardi, N., and S. Fagherazzi. 2014. How waves shape salt marshes. Geology **42**: 887–890. doi:10.1130/G35751.1.

Leonardi, N., N. K. Ganju, and S. Fagherazzi. 2016. A linear relationship between wave power and erosion determines salt-marsh resilience to violent storms and hurricanes. Proc. Natl. Acad. Sci. USA **113**: 64–68. doi:10.1073/pnas.1510095112.

Liu, W., D. R. Strong, S. C. Pennings, and Y. Zhang. 2017. Provenance-by-environment interaction of reproductive traits in the invasion of *Spartina alterniflora* in China. Ecology **98**: 1591–1599. doi:10.1002/ecy.1815.

Marani, M., A. D'Alpaos, S. Lanzoni, and M. Santalucia. 2011. Understanding and predicting wave erosion of marsh edges. Geophys. Res. Lett. **38**: L21401. doi:10.1029/2011GL048995.

Marion, S. R., and R. J. Orth. 2012. Seedling establishment in eelgrass: Seed burial effects on winter losses of developing seedlings. Mar. Ecol. Prog. Ser. **448**: 197–207. doi:10.3354/meps09612.

Mariotti, G., and S. Fagherazzi. 2010. A numerical model for the coupled long-term evolution of salt marshes and tidal flats. J. Geophys. Res. **115**: F01004. doi:10.1029/2009JF001326.

Mariotti, G., and S. Fagherazzi. 2013. Critical width of tidal flats triggers marsh collapse in the absence of sea-level rise. Proc. Natl. Acad. Sci. USA **110**: 5353–5356. doi:10.1073/pnas.1219600110

Mendelssohn, I. A., and N. L. Kuhn. 2003. Sediment subsidy: Effects on soil–plant responses in a rapidly submerging coastal salt marsh. Ecol. Eng. **21**: 115–128. doi:10.1016/j.ecoleng.2003.09.006.

Nehring, S., and K.-J. Hesse. 2008. Invasive alien plants in marine protected areas: The *Spartina anglica* affair in the European Wadden Sea. Biol. Invasions **10**: 937–950. doi:10.1007/s10530-008-9244-z.

Paramor, O. A. L., and R. G. Hughes. 2004. The effects of bioturbation and herbivory by the polychaete *Nereis diversicolor* on loss of saltmarsh in south-east England. J. Appl. Ecol. **41**: 449–463. doi:10.1111/j.0021-8901.2004.00916.x.

Pontee, N. 2013. Defining coastal squeeze: A discussion. Ocean Coast. Manag. **84**: 204–207. doi:10.1016/j.ocecoaman.2013.07.010.

Scyphers, S. B., S. P. Powers, K. L. Heck Jr., and D. Byron. 2011. Oyster reefs as natural breakwaters mitigate shoreline loss and facilitate fisheries. PLoS One **6**: e22396. doi:10.1371/journal.pone.0022396.

Silliman, B. R., and others. 2012. Degradation and resilience in Louisiana salt marshes after the BP–*Deepwater Horizon* oil spill. Proc. Natl. Acad. Sci. USA **109**: 11234–11239. doi:10.1073/pnas.1204922109.

Sistermans, P., and O. Nieuwenhuis. 2019. Western scheldt estuary (The Netherlands). EUROSION Case Study. http://databases.eucc-d.de/plugins/projectsdb/project.php?show=380

Strong, D. R., and D. R. Ayres. 2013. Ecological and evolutionary misadventures of *Spartina*. Annu. Rev. Ecol. Evol. Syst. **44**: 389–410. doi:10.1146/annurev-ecolsys-110512-135803.

Suykerbuyk, W., and others. 2016. Surviving in changing seascapes: Sediment dynamics as bottleneck for long-term seagrass presence. Ecosystems **19**: 296–310. doi:10.1007/s10021-015-9932-3.

Swart, D. 1977. Predictive equations regarding coastal transports, p. 1113–1132. *In* Johnson, J. W. (ed.), Proceedings of the 15th Coastal Engineering Conference held at Honolulu, Hawaii, USA from 11-17 July 1976, ASCE, Vol. II.

Syvitski, J. P. M., and others. 2009. Sinking deltas due to human activities. Nat. Geosci. **2**: 681–686. doi:10.1038/ngeo629.

Temmerman, S., T. Bouma, J. Van de Koppel, D. Van der Wal, M. De Vries, and P. Herman. 2007. Vegetation causes channel erosion in a tidal landscape. Geology **35**: 631–634. doi:10.1130/G23502A.1.

Temmerman, S., P. Meire, T. J. Bouma, P. M. J. Herman, T. Ysebaert, and H. J. De Vriend. 2013. Ecosystem-based

coastal defence in the face of global change. Nature **504**: 79–83. doi:10.1038/nature12859.

Tucker, M. J., and E. G. Pitt. 2001. Waves in ocean engineering. Elsevier ocean engineering book series, v. **5**. Elsevier.

van de Koppel, J., D. van der Wal, J. P. Bakker, and P. M. Herman. 2005. Self-organization and vegetation collapse in salt marsh ecosystems. Am. Nat. **165**: E1–E12. doi:10.1086/426602.

van der Wal, D., and K. Pye. 2004. Patterns, rates and possible causes of saltmarsh erosion in the Greater Thames area (UK). Geomorphology **61**: 373–391. doi:10.1016/j.geomorph.2004.02.005

van der Wal, D., A. Wielemaker-Van den Dool, and P. M. J. Herman. 2008. Spatial patterns, rates and mechanisms of saltmarsh cycles (Westerschelde, The Netherlands). Estuar. Coast. Shelf Sci. **76**: 357–368. doi:10.1016/j.ecss.2007.07.017.

van Rijn, L. C. 1993. Principles of sediment transport in rivers, estuaries and coastal seas. Aqua Publication.

van Wesenbeeck, B. K., J. van de Koppel, P. M. J. Herman, J. P. Bakker, and T. J. Bouma. 2007. Biomechanical warfare in ecology; negative interactions between species by habitat modification. Oikos **116**: 742–750. doi:10.1111/j.0030-1299.2007.15485.x.

Walling, D. E., and D. Fang. 2003. Recent trends in the suspended sediment loads of the world's rivers. Glob. Planet. Chang. **39**: 111–126. doi:10.1016/S0921-8181(03)00020-1.

Wang, H., and others. 2017. Zooming in and out: Scale dependence of extrinsic and intrinsic factors affecting salt marsh erosion. J. Geophys. Res. **122**: 1455–1470. doi:10.1002/2016JF004193.

Wolters, M., and J. P. Bakker. 2002. Soil seed bank and driftline composition along a successional gradient on a temperate salt marsh. Appl. Veg. Sci. **5**: 55–62. doi:10.1111/j.1654-109X.2002.tb00535.x.

Xiao, D., L. Zhang, and Z. Zhu. 2009. A study on seed characteristics and seed bank of *Spartina alterniflora* at saltmarshes in the Yangtze estuary, China. Estuar. Coast. Shelf Sci. **83**: 105–110. doi:10.1016/j.ecss.2009.03.024.

Xiao, D., L. Zhang, and Z. Zhu. 2010. The range expansion patterns of *Spartina alterniflora* on salt marshes in the Yangtze Estuary, China. Estuar. Coast. Shelf Sci. **88**: 99–104. doi:10.1016/j.ecss.2010.03.015.

Yang, S. L., and others. 2008. Spatial and temporal variations in sediment grain size in tidal wetlands, Yangtze Delta: On the role of physical and biotic controls. Estuar. Coast. Shelf Sci. **77**: 657–671. doi:10.1016/j.ecss.2007.10.024.

Zhu, Z., L. Zhang, N. Wang, C. Schwarz, and T. Ysebaert. 2012. Interactions between the range expansion of saltmarsh vegetation and hydrodynamic regimes in the Yangtze Estuary, China. Estuar. Coast. Shelf Sci. **96**: 273–279. doi:10.1016/j.ecss.2011.11.027.

Zhu, Z., T. J. Bouma, T. Ysebaert, L. Zhang, and P. M. J. Herman. 2014. Seed arrival and persistence at the tidal mudflat: Identifying key processes for pioneer seedling establishment in salt marshes. Mar. Ecol. Prog. Ser. **513**: 97–109. doi:10.3354/meps10920.

Zhu, Z., and others. 2016. Sprouting as a gardening strategy to obtain superior supplementary food: Evidence from a seed-caching marine worm. Ecology **97**: 3278–3284. doi:10.1002/ecy.1613.

Acknowledgment

We are grateful to Lennart van IJzerloo, Jeroen van Dalen, Nanyang Chu, and Artis Vansovics for their assistances in the field. We also thank Valarie de Witte for her help in checking the grammar. Z.Z. and T.J.B. were funded by the BE-SAFE project (grant 850.13.011) financed by the Netherlands Organization for Scientific Research (NWO). Z.Z. was also supported by the project funded by China Postdoctoral Science Foundation (2019M652825). J.v.B. and J.v.d.K. were supported by the VNSC project "Vegetation modeling HPP" (contract 3109 1805).

Conflict of Interest

None declared.

Submitted 16 January 2019
Revised 27 May 2019
Accepted 14 June 2019

Associate editor: K. David Hambright